

Supporting Information

Shape-tuned Diamond-Hexagonal Semiconductor Nanocones

Linyou Cao¹, Lee Laim¹, Chaoying Ni², Bahram Nabet^{1,3,4}, and Jonathan E. Spanier^{1,3,4,*}

¹*Department of Materials Science and Engineering, Drexel University, Philadelphia PA 19104,* ²*W. M.*

Keck Electron Microscopy Facility, University of Delaware, Newark DE 19716, ³*Department of*

Electrical and Computer Engineering, Drexel University, Philadelphia PA 19104, ⁴*A. J. Drexel*

Nanotechnology Institute, Drexel University, Philadelphia PA 19104

*Author to whom correspondence should be addressed: spanier@drexel.edu

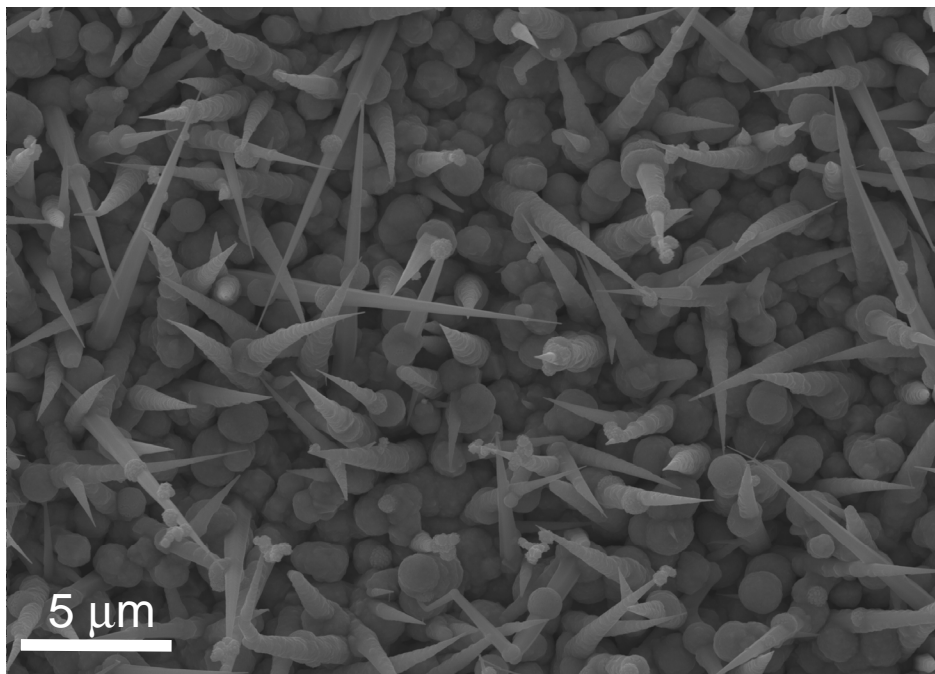


Figure 4. Scanning electron microscopy image of germanium nanocones (GeNCs).

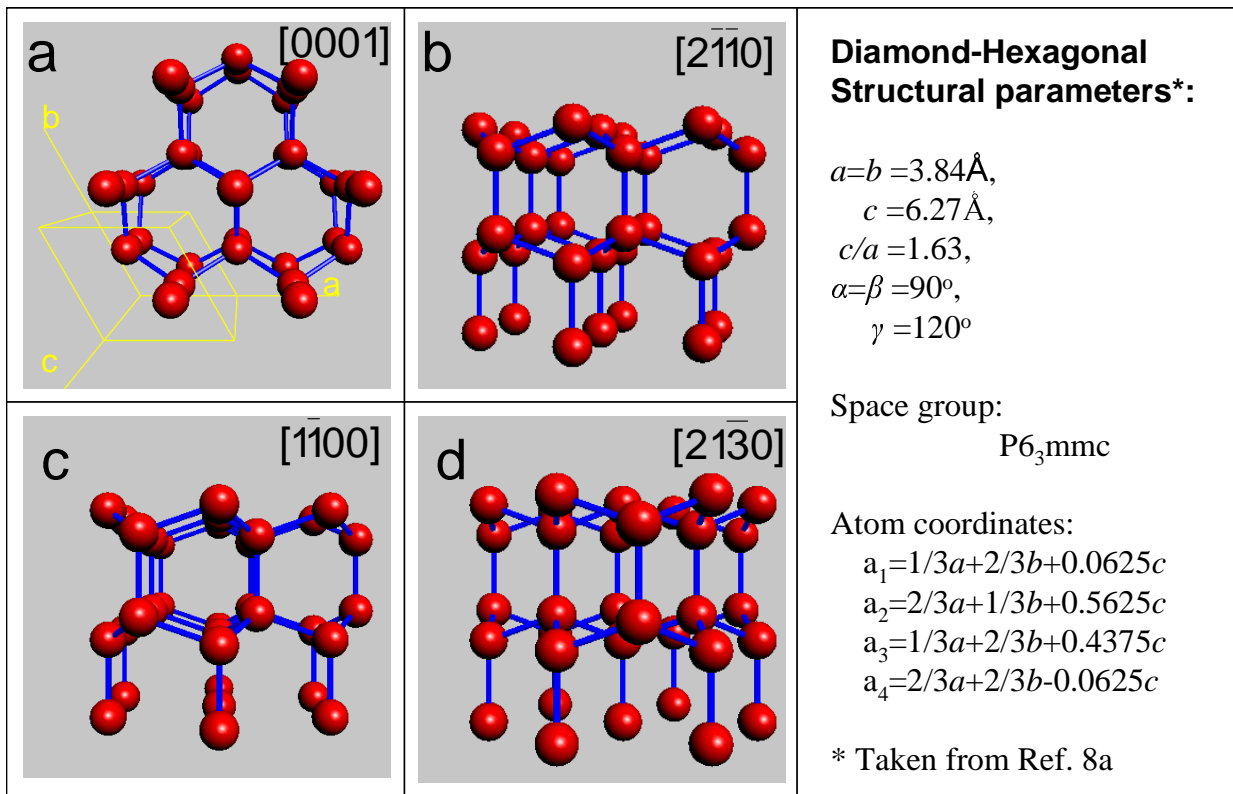


Figure 5. Structural model for DH silicon with different view directions of (a) [0001], (b) [2110], (c) [1100], and (d) [2130], as denoted in the figures. The yellow polyhedron in (a) shows coordinates of a , b , c and the primitive cell. The structural parameters of diamond-hexagonal silicon phase are also given in the panel on the right and are taken from Ref. 8a in the main text.

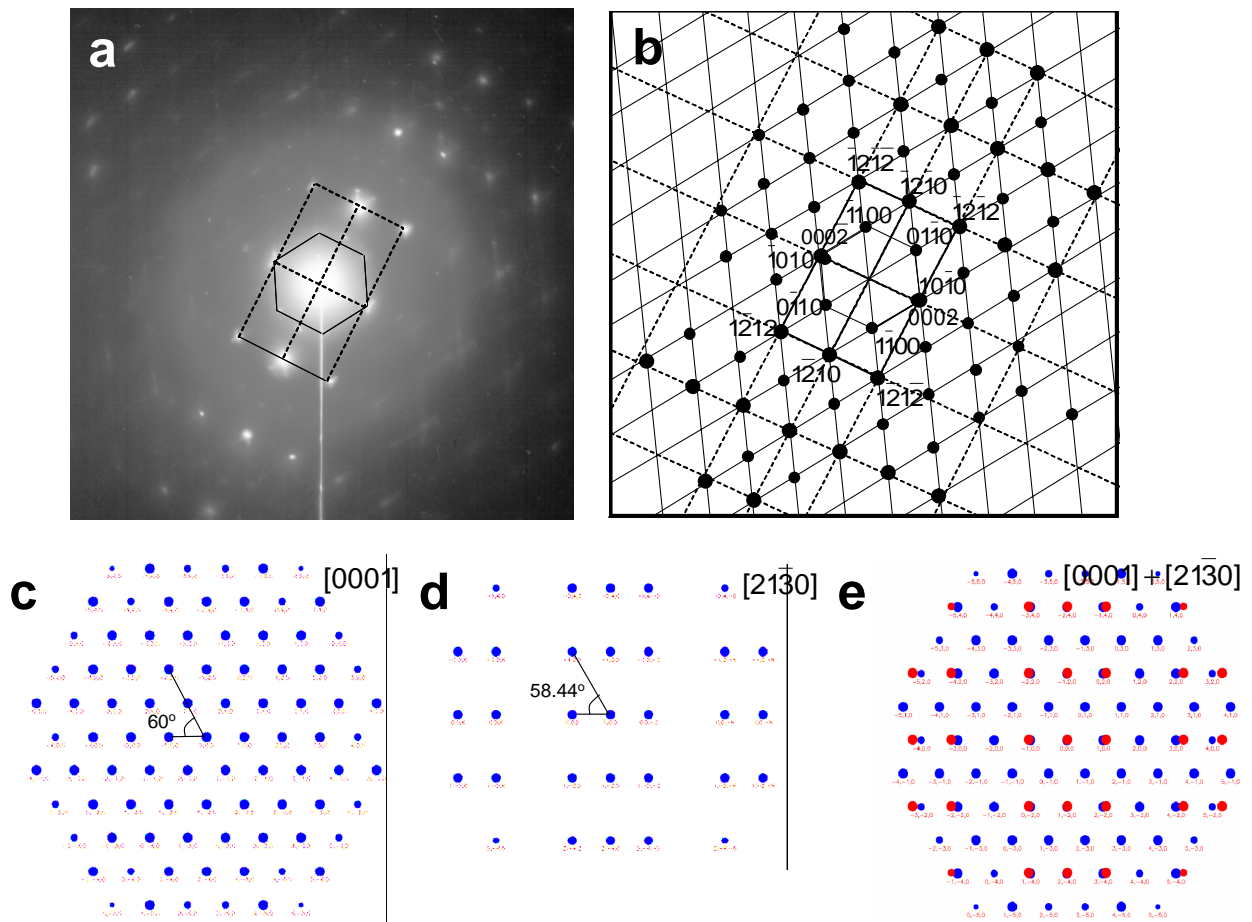


Figure 6. (a) Electron diffraction pattern of Fig. 2b in the main text and (b) the corresponding schematic figure for indexing showing the superposition of $[0001]$ and $[21\bar{3}0]$ zone axes diffraction patterns with common $\langle \bar{1}2\bar{1}0 \rangle$ reflections. Also shown are simulated electron diffraction patterns of (c) $[0001]$ and (d) $[21\bar{3}0]$ zone axes as well as (e) their superposition with common $\langle \bar{1}2\bar{1}0 \rangle$ reflections.

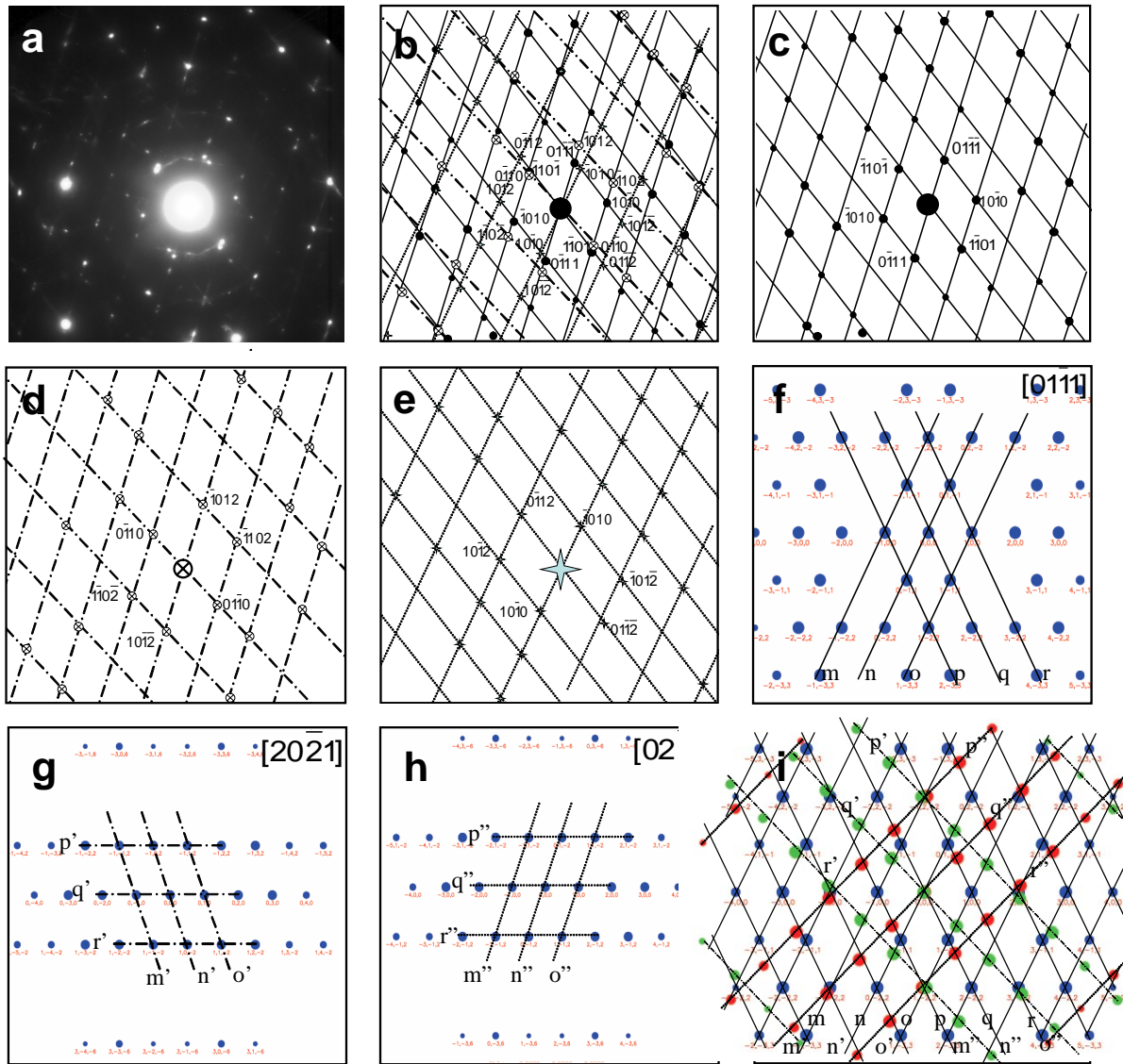


Figure 7. (a) Electron diffraction pattern of Fig. 2d, and (b) corresponding schematic figure for indexing showing the superposition of one $[01\bar{1}1]$ and two $[201]$ zone axis diffraction patterns, as well as schematic figures for the (c) $[01\bar{1}1]$, (d) $[20\bar{2}1]$, and (e) $[02\bar{2}1]$ zone patterns. Also shown are simulated electron diffraction patterns for (f) $[01\bar{1}1]$, (g) $[20\bar{2}1]$, (h) and $[02\bar{2}1]$ zone axes, and (i) the superposition of (f)-(h). The indexed lines m-r, m'-r', m''-r'' are included to

clarify how patterns (f)-(h) are superimposed. Briefly, the lines m-o in (f) are collinear with m'-o' in (g), respectively, and lines p-r in (f) are collinear with m''-o'' in (h), respectively. It should be noted that the experimental [201] zone patterns (d)-(e) differ to some extent from the simulated results (g)-(h); this is likely due to the deviation of the electron beam from the normal direction of sample plane.

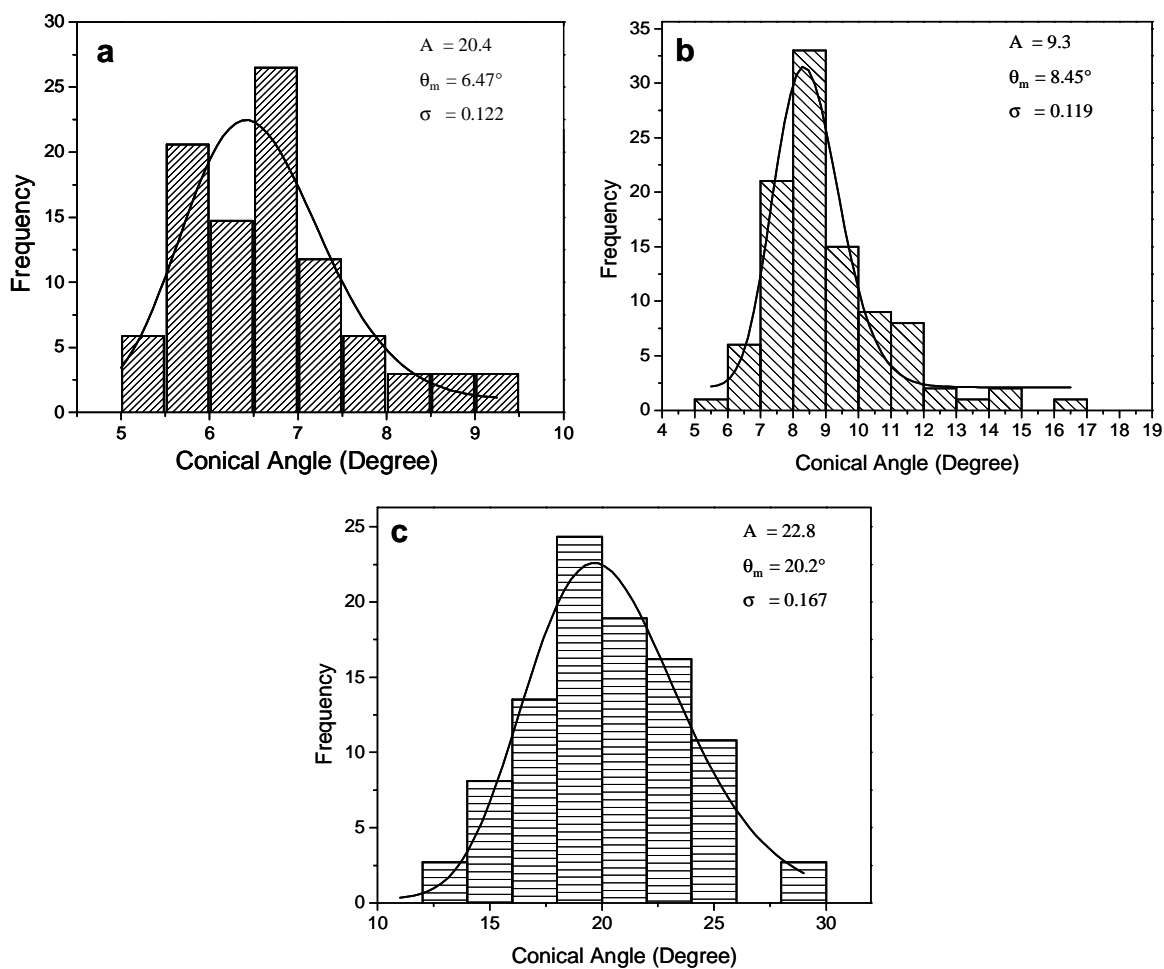


Figure 8. Histograms of conical angles of SiNCs produced using catalyst diameters (a) 50 nm, (b) 20 nm and (c) 2 nm. Also shown is the result of a log-normal fitting of each, along with the fitting parameters.